Superior biocompatible carbon dots for dynamic fluorescence imaging of nucleolus in living cells

Liyun Lin[1,#], Zhouzhou Bao[2,3,#], Pengfei Jiang[1], Zhourui Xu[4], Bo Shi[5], Gaixia Xu[4,*], Dan Wang[5,*], Xunbin Wei[6,*], Bobo Gu[1,*]

[1]Med-X Research Institute and School of Biomedical Engineering, Shanghai Jiao Tong University, Shanghai 200030, China
[2]Department of Obstetrics and Gynecology, Ren Ji Hospital, School of Medicine, Shanghai Jiao Tong University, Shanghai, China
[3]Shanghai Key Laboratory of Gynecologic Oncology, Ren Ji Hospital, School of Medicine, Shanghai Jiao Tong University, Shanghai, China
[4]Guangdong Key Laboratory for Biomedical Measurements and Ultrasound Imaging, School of Biomedical Engineering, Health Science Center, Shenzhen University, Shenzhen, Guangdong 518055, China
[5]State Key Laboratory of Organic Inorganic Composites, Beijing University of Chemical Technology, Beijing, 100029, China
[6]Biomedical Engineering Department and International Cancer Institute, Peking University, Beijing 100081, China
#: These authors contributed equally

*E-mail: xugaixia@szu.edu.cn (Gaixia Xu), wangdan@mail.buct.edu.cn (Dan Wang), xwei@bjmu.edu.cn (Xunbin Wei), bobogu@sjtu.edu.cn (Bobo Gu)

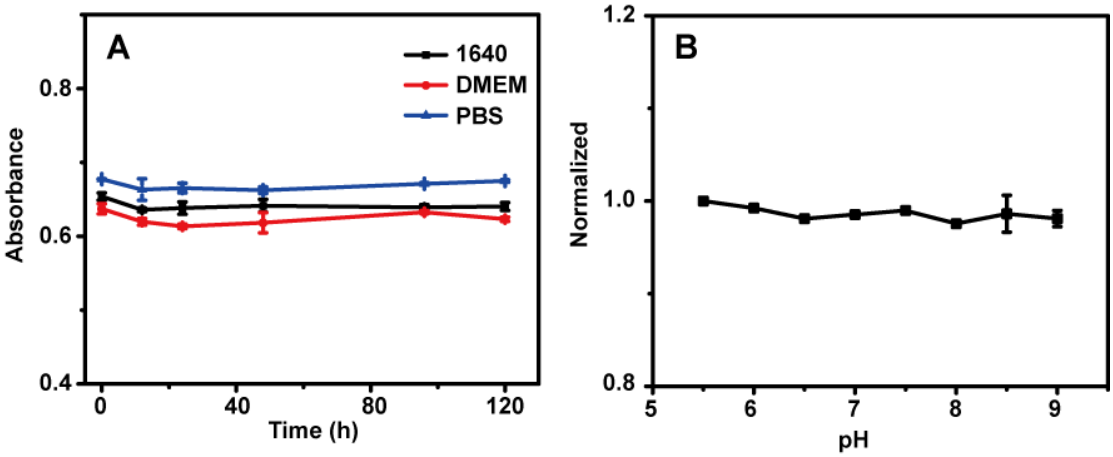

Fig. S1. (A) Long-term stability of CDs in PBS and cell medium. (B) The fluorescence intensity of the CDs in different pH solutions (n=3).

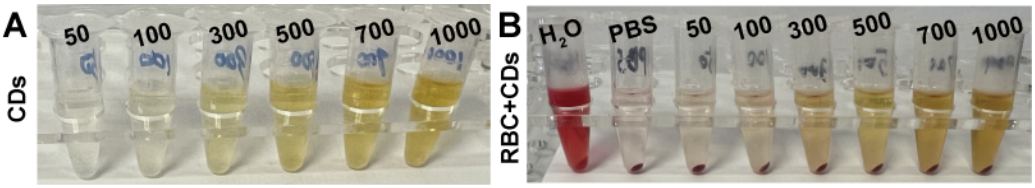

Fig. S2. The photograph of (A) various concentrations of CDs (50-1000 μg mL^{-1}, without RBCs) and (B) RBCs cultured with H_2O, PBS, various concentrations of CDs for 12 h.

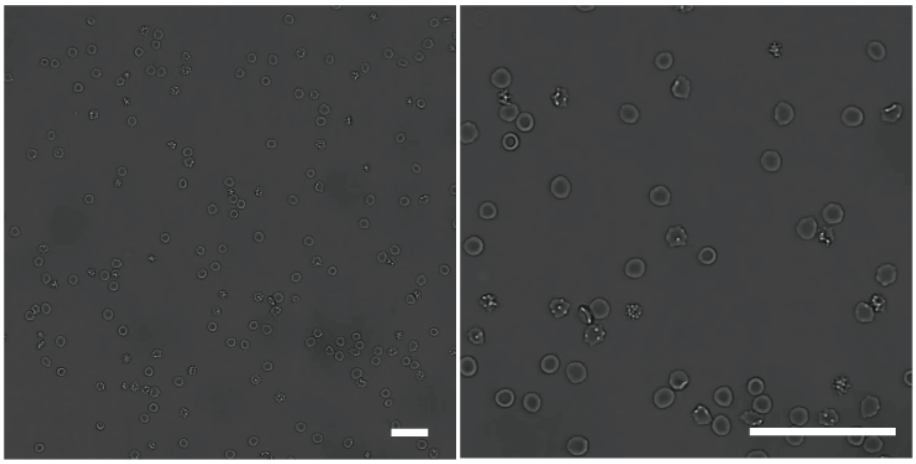

Fig. S3. Photos of RBCs cultured with CDs for 24 h under bright field. Scale bar: 100 μm.

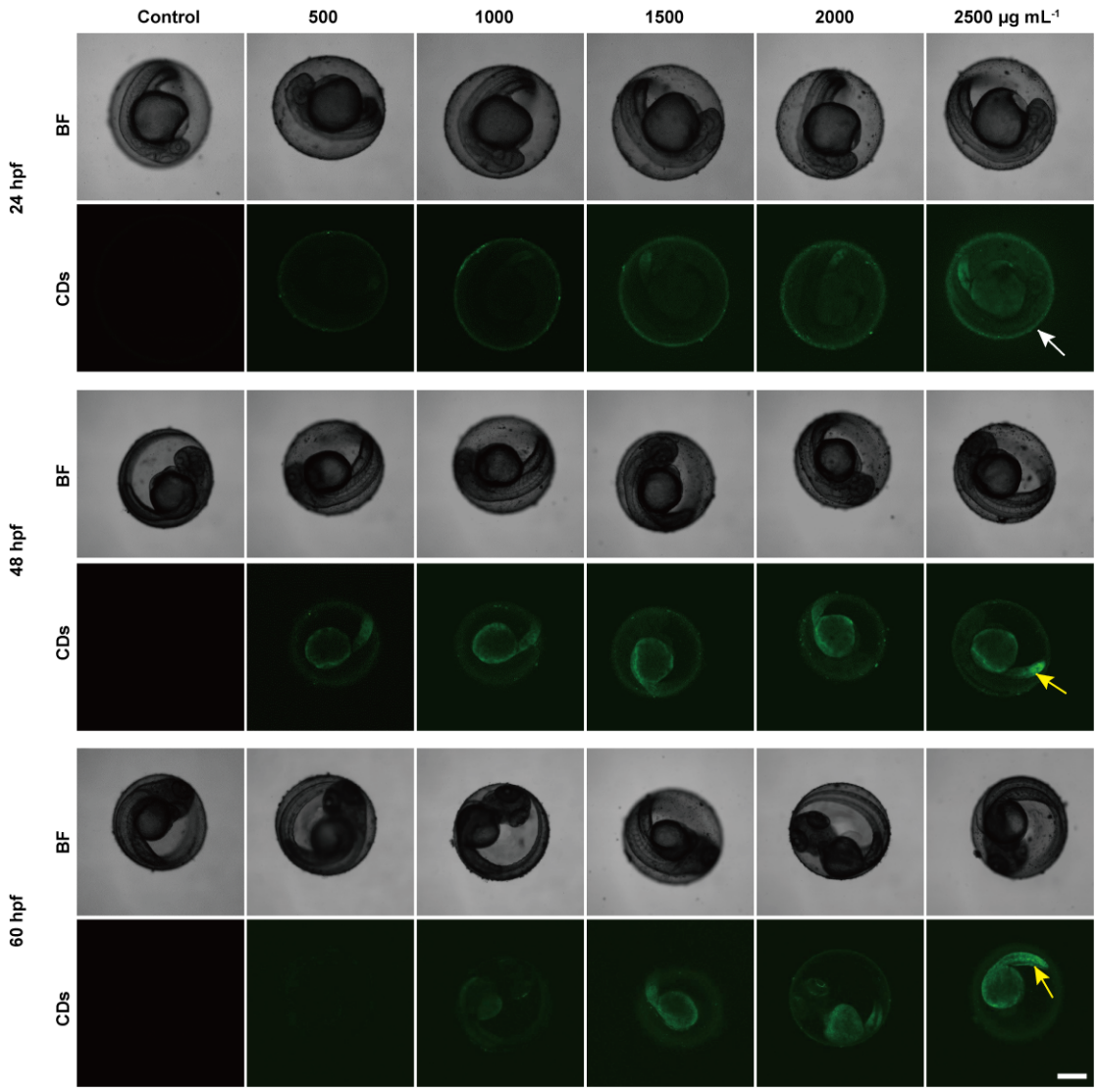

Fig. S4. Bright field and fluorescence images of zebrafish embryos at different periods (24, 48, 60 hpf) after soaking in different concentrations CDs solutions for 12 h. 5× objective lens was used. BF: bright field. Scale bars: 100 μm.

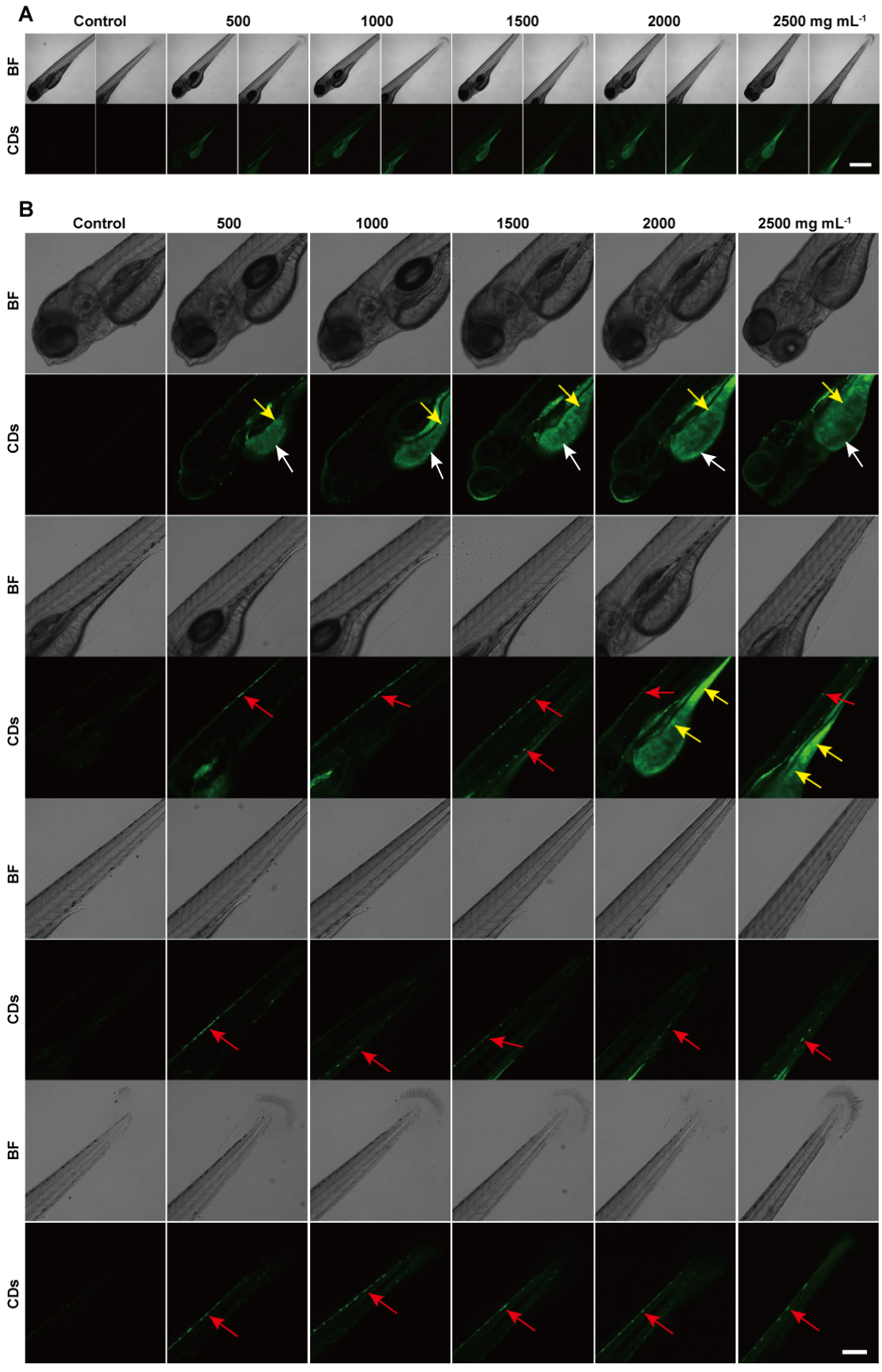
A
Control
500
1000
1500
2000
2500 mg mL-1
BF
CDs
B
Control
500
1000
1500
2000
2500 mg mL-1
BF
CDs
BF
CDs
BF
CDs
BF
CDs

Fig. S5. Bright field and fluorescence images of (A) whole bodies, and (B) enlarged head, yolk sac, trunk and tail of zebrafish larvae at 72 hpf after soaking for 12 h in CDs solution of different concentrations. White, red and yellow arrows indicated the yolk sac, blood vessel and intestine, respectively. A 5× objective lens was used for (A) and a 10× objective lens was used for (B). BF: bright field. Scale bars: 400 μm for (A) and 200 μm for (B).

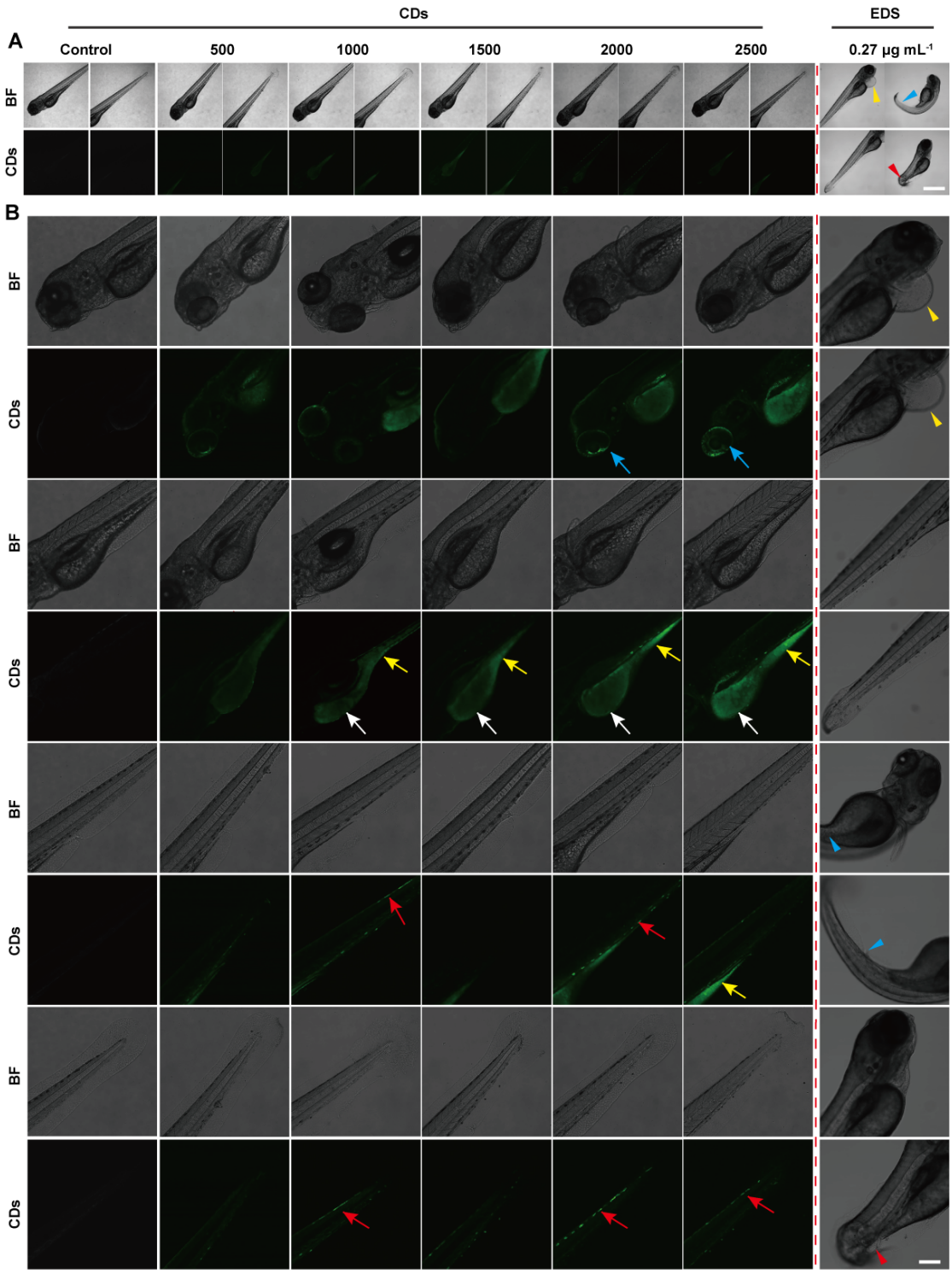

Fig. S6. Bright field and fluorescence images of (A) whole bodies, positive group (right column) and (B) enlarged images of head, yolk sac, trunk and tail of zebrafish larvae at 96 hpf after soaking for 12 h in CDs solution of different concentrations. White, red and yellow arrows indicated the yolk sac, blood vessel and intestine, respectively. Yellow, blue and red triangle indicated the

pericardial edema, deformed tail, and docked tail, respectively. A 5x objective lens was used for (A) and a 10x objective lens was used for (B). BF: bright field. Scale bars: 400 μm for (A) and 200 μm for (B).

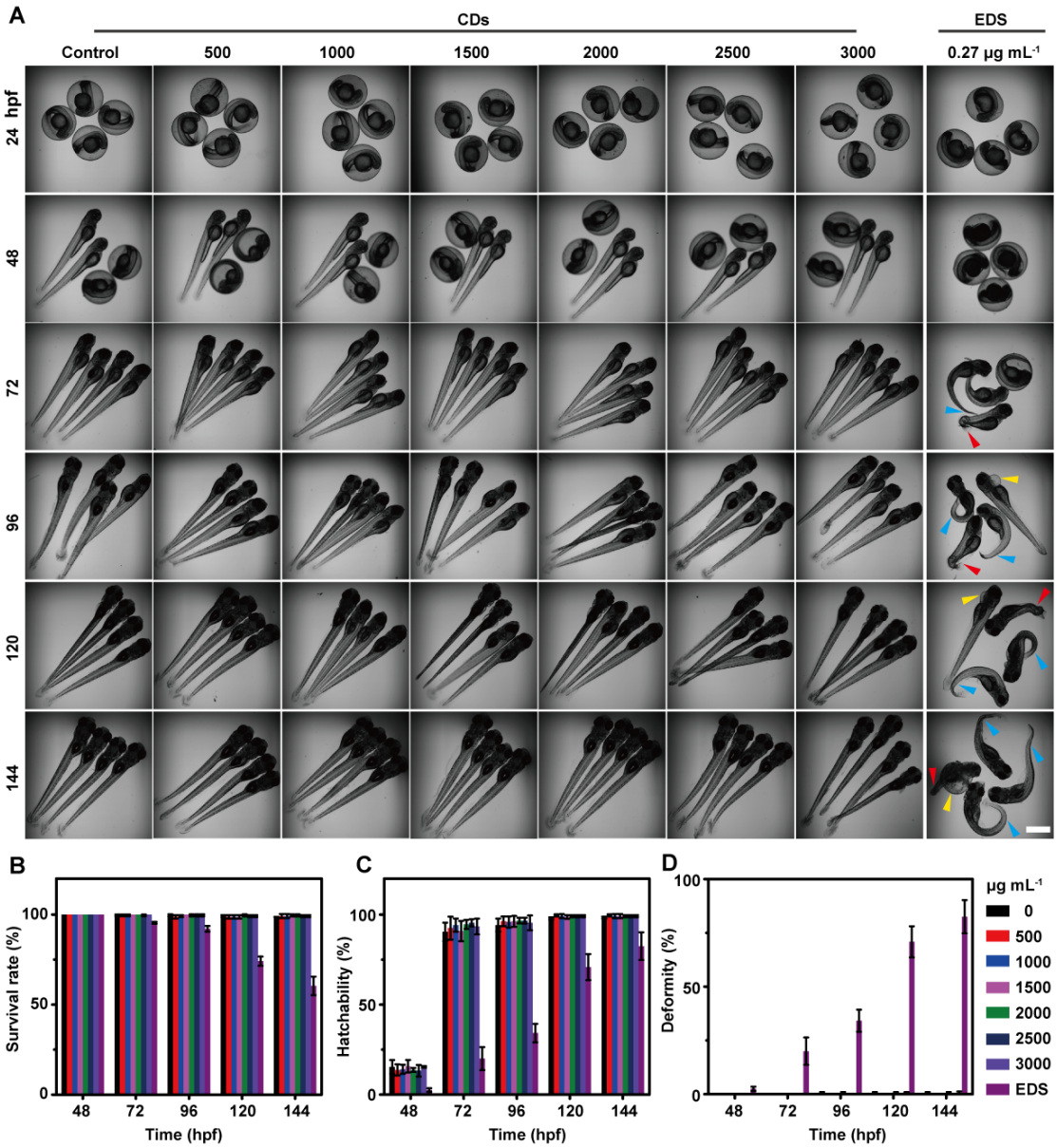

Fig. S7. (A) Representative bright field images of embryos and larvae incubated with various concentration CDs and 10 μM EDS (0.27 μg mL^{-1}, i.e., positive group) which were obtained through a 2.5x dry objective at 24 h intervals for six consecutive days. Yellow, blue and red triangle indicated the pericardial edema, deformed tail, and docked tail, respectively. Scale bar: 400 μm. The corresponding (B) survival ratio, (C) hatchability and (D) deformity of embryos and larvae.

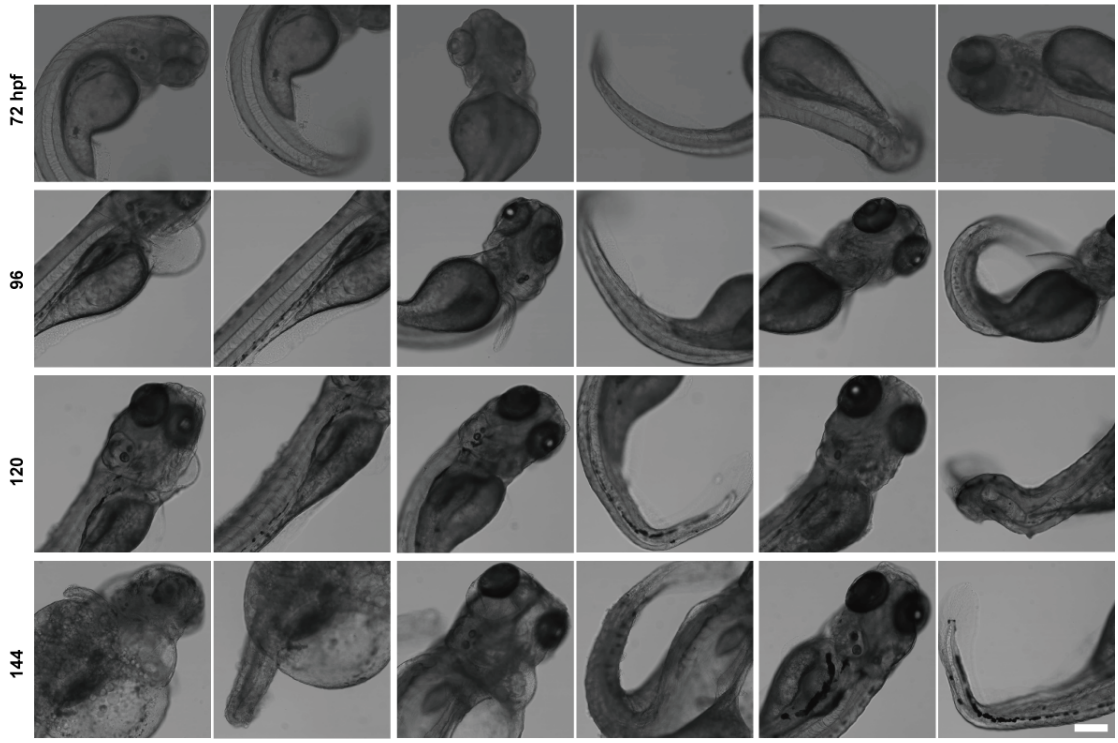

Fig. S8. Enlarged bright field images of head, yolk sac, trunk and tail of zebrafish larvae at 72-144 hpf after incubating for 12 h in EDS solution (10 μM, 0.27 μg mL^{-1}). A 10x objective lens was used for imaging. Scale bars: 200 μm.

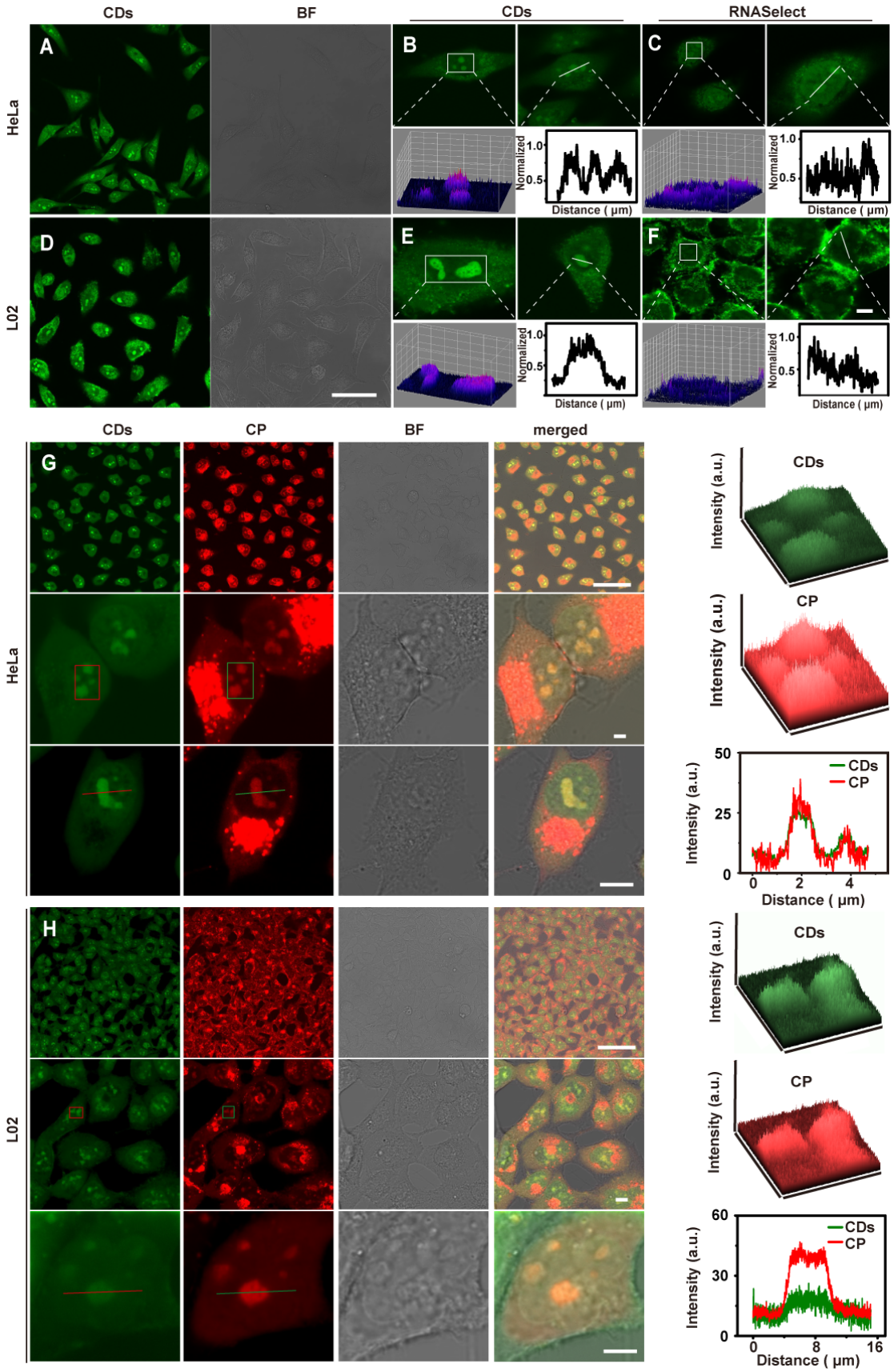
CDs
BF
CDs
RNASelect
HeLa
L02
A
B
C
D
E
F
Normalized
1.0
0.5
Distance (μm)
CDs
CP
BF
merged
G
H
Intensity (a.u.)
50
25
0
0
2
4
60
30
0
8
16

Fig. S9. Fluorescence imaging of nucleoli using CDs. Confocal fluorescence images, distribution and fluorescence intensity profile of enlarged nucleoli region of (A-C) HeLa cells and (D-F) L02 cells treated with the CDs and RNASelect. Fluorescence images of (G) HeLa and (H) L02 cells stained with both CDs and CP, and corresponding bright field, merged images, distribution of selected region and fluorescence intensity profile in enlarged nucleoli region. CDs channel (Ex: 488 nm, Em: 500-540 nm), CP channel (Ex: 552 nm, Em: 600-690 nm), RNASelect channel (Ex: 488 nm, Em: 510-540 nm). CP: 15 μM, CDs: 200 μg mL^{-1}. Scale bar: 50 μm for entire images, 5 μm for enlarged images.

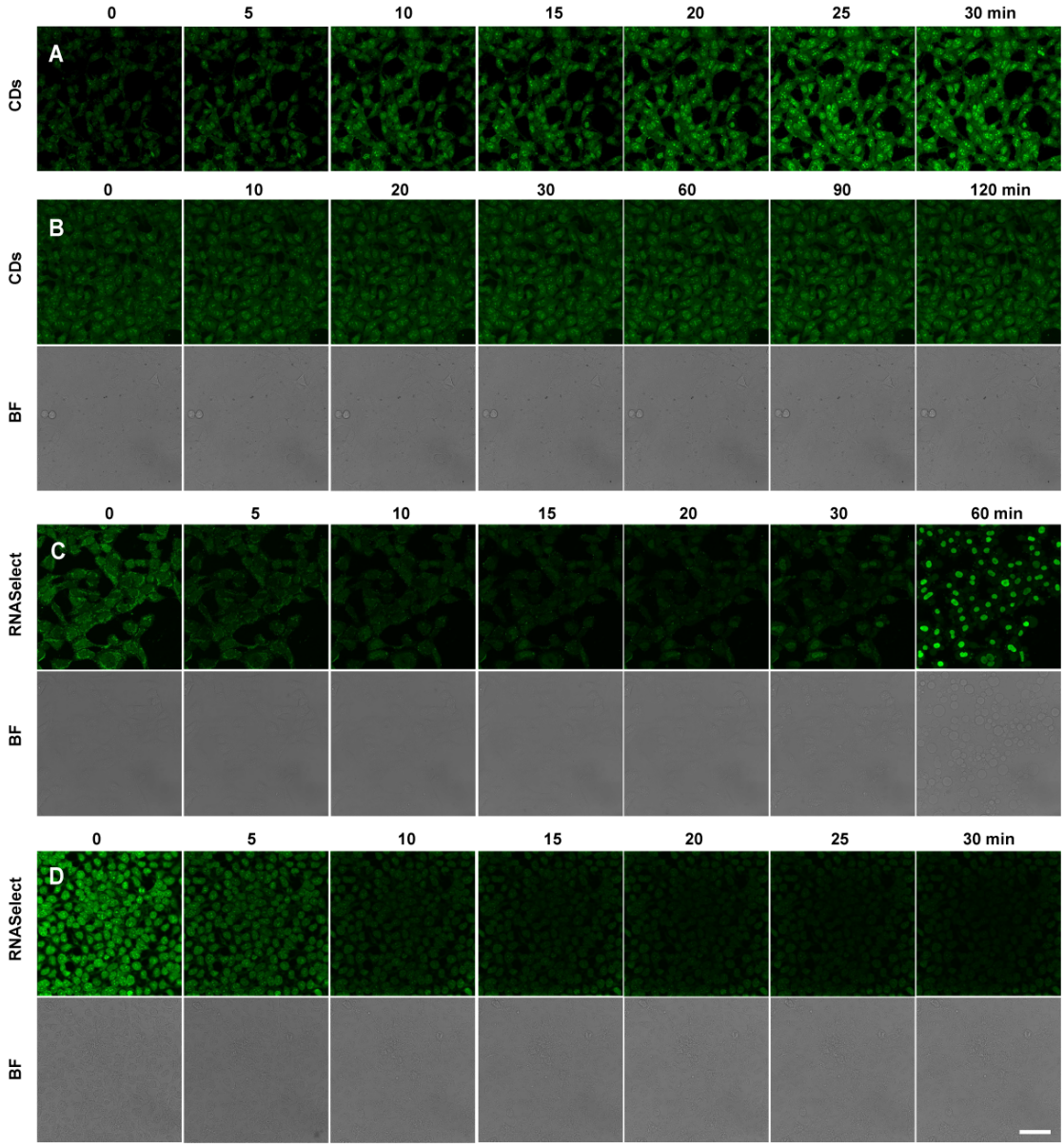

Fig. S10. Long-term imaging of nucleoli in L02 cells using CDs. (A) Time-dependent cellular internalization of CDs within 30 min. Images of (B) CDs and (C) RNASelect-stained living cells after continuous irradiation (488 nm) for different time periods. (D) Images of RNASelect-stained fixed cells after continuous irradiation (488 nm) for different time periods. CDs channel (Ex: 488 nm, Em: 500-540 nm), RNASelect channel (Ex: 488 nm, Em: 510-540 nm). RNASelect: 5 μM, CDs: 200 μg mL^{-1}. Scale bar: 50 μm.

Table S1 Hematological parameters of the mice untreated, treated with CDs at day 3, 14, and the reference ranges of normal mice.

Parameters	Day	Control	Low dose	High Dose	Ref
ALB	3	24.83±1.15	23.68±2.0	23.73±2.66	21.22-39.15
(g L^{-1})	14	25.06±1.04	24.28±0.32	23.28±1.96	
AST	3	107.8±2.41	110.16±12.52	136.17±19.40	36.31-235.48
(U L^{-1})	14	104.50±6.33	108.78±11.32	122.06±19.09	
ALT	3	13.80±2.95	25.26±3.30	29.90±4.18	10.06-96.47
(U L^{-1})	14	14.38±4.21	29.12±4.76	20.16±6.40	
TP	3	59.60±1.06	57.52±3.27	59.27±2.75	38.02-75.06
(g L^{-1})	14	59.58±1.76	59.08±1.80	58.20±2.24	
CREA	3	14.63±5.75	23.34±3.80	16.4±7.18	10.91-85.09
(μM)	14	13.38±5.24	13.63±3.77	10.0±2.26	
Glu	3	7.22±0.31	6.99±1.44	7.49±0.66	4.66-13.42
(mM)	14	6.47±1.15	7.18±1.02	6.56±0.63	
Lymph#	3	3.16±0.40	3.08±0.58	1.84±0.59	0.7-5.7
(10^9 L^{-1})	14	3.30±0.16	3.44±0.58	0.76±0.22	
Mon#	3	0.06±0.05	0.10±0	0.02±0.04	0.0-0.3
(10^9 L^{-1})	14	0.06±0.05	0.04±0.05	0.04±0.05	
WBC	3	4.08±0.45	3.66±0.65	2.22±0.64	0.8-6.8
(10^9 L^{-1})	14	4.08±0.16	4.42±0.73	1.0±0.32	
MCV	3	52.98±1.06	53.02±1.18	52.46±0.63	48.2-58.3
(fL)	14	53.68±0.90	54.92±0.38	53.92±0.34	
MCH	3	15.78±0.46	15.78±0.41	15.20±0.36	15.8-19.0
(pg)	14	16.18±0.35	15.92±0.15	14.96±0.17	
RDW	3	13.18±0.97	13.82±1.36	13.38±0.51	13.0-17.0
(%)	14	13.92±0.65	14.76±0.36	13.50±0.90	

Table S2 Summary of representative toxicological studies of various nanomaterials.

NPs	Size (nm)	In Vitro ($mg \cdot mL^{-1}$)	Dose	Distribution	Animal Model	Toxicological responses	Ref
Mg-MOF-74	250-350	0.5	2 mg mL^{-1}	Lung, heart, kidney	Mouse	Cells morphologies distinct change	1
PCN-22	200	160	5 mg kg^{-1}	Lung, kidney, liver	Mouse	-	2
Uio-66(Zr)	50-90	200	50 mg kg^{-1}	Liver, Spleen	Mouse	-	3
CuO	18±5	-	0.5 $mg \cdot mL^{-1}$	-	Zebrafish embryo/larva	*	4
NiO	40±12	-	0.5 $mg \cdot mL^{-1}$	-	Zebrafish embryo/larva	*	4
ZnO	23±7	-	0.5 $mg \cdot mL^{-1}$	-	Zebrafish embryo/larva	*	4
MWCNTs	(8-15)* (10000-50000)	-	20 $\mu g \cdot mL^{-1}$	-	Zebrafish embryo/larva	*	5
GO nanosheets	96	-	0.25 $mg \cdot mL^{-1}$	-	Zebrafish embryo/larva	Developmental toxicity	6
Si QDs	5-10	-	0.1-0.8 $\mu g \cdot mL^{-1}$	-	Zebrafish embryo	Death or abnormality	7
UCNPs	17	-	0.005-5 nM	-	Zebrafish embryo	Growth retardation, heart deformity, and bent tail	8
Ag NPs	20-110	-	1-5 $\mu g \cdot mL^{-1}$	-	Adult Zebrafish	Toxic to gills and intestines	9
Au NPs	50	-	0-20 $\mu g \cdot mL^{-1}$	-	Zebrafish embryo	Epidermal toxicity	10
CDs	10	-	10 $\mu g \cdot mL^{-1}$	-	Zebrafish embryo/larva	No	11
CDs	4.2	0-1.5	0-3 mg mL^{-1}	Kidney, Lung	Mouse and Zebrafish embryo/larva	No	This work

* Death, hatching delay, decreased heartbeat rates, and abnormalities

Reference:

1. Zhu Z, Jiang S, Liu Y, et al. Micro or nano: Evaluation of biosafety and biopotency of magnesium metal organic framework-74 with different particle sizes[J]. Nano Research, 2020, 13(2): 511-526.

2. Cheng Q, Yu W, Ye J, et al. Nanotherapeutics interfere with cellular redox homeostasis for highly improved photodynamic therapy[J]. Biomaterials, 2019, 224: 119500.

3. Chen D, Yang D, Dougherty C A, et al. In vivo targeting and positron emission tomography imaging of tumor with intrinsically radioactive metal-organic frameworks nanomaterials[J]. ACS Nano, 2017, 11(4): 4315-4327.

4. Lin S, Zhao Y, Xia T, et al. High content screening in zebrafish speeds up hazard ranking of transition metal oxide nanoparticles[J]. ACS Nano, 2011, 5(9): 7284-7295.

5. Aksakal F I, Ciltas A, Ozek N S. A holistic study on potential toxic effects of carboxylated multi-walled carbon nanotubes (MWCNTs-COOH) on zebrafish (Danio rerio) embryos/larvae[J]. Chemosphere, 2019, 225: 820-828.

6. Jeong J, Cho H J, Choi M, et al. In vivo toxicity assessment of angiogenesis and the live distribution of nano-graphene oxide and its PEGylated derivatives using the developing zebrafish embryo[J]. Carbon, 2015, 93: 431-440.

7. Fan J W, Vankayala R, Chang C L, et al. Preparation, cytotoxicity and in vivo bioimaging of highly luminescent water-soluble silicon quantum dots[J]. Nanotechnology, 2015, 26(21): 215703.

8. Jang G H, Hwang M P, Kim S Y, et al. A systematic in-vivo toxicity evaluation of nanophosphor particles via zebrafish models[J]. Biomaterials, 2014, 35(1): 440-449.

9. Osborne O J, Lin S, Chang C H, et al. Organ-specific and size-dependent Ag nanoparticle toxicity in gills and intestines of adult zebrafish[J]. ACS Nano, 2015, 9(10): 9573-9584.

10. Jia H R, Zhu Y X, Xu K F, et al. Efficient cell surface labelling of live zebrafish embryos: wash-free fluorescence imaging for cellular dynamics tracking and nanotoxicity evaluation[J]. Chemical Science, 2019, 10(14): 4062-4068.